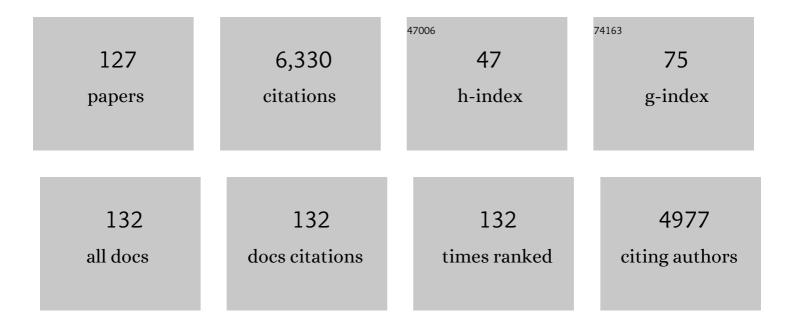
Richard Aster

List of Publications by Year in descending order

Source: https://exaly.com/author-pdf/2788099/publications.pdf Version: 2024-02-01



#	Article	IF	CITATIONS
1	Radial Anisotropy and Sediment Thickness of West and Central Antarctica Estimated From Rayleigh and Love Wave Velocities. Journal of Geophysical Research: Solid Earth, 2022, 127, .	3.4	7
2	Shear Wave Splitting Across Antarctica: Implications for Upper Mantle Seismic Anisotropy. Journal of Geophysical Research: Solid Earth, 2022, 127, .	3.4	3
3	Teleseismic earthquake wavefields observed on the Ross Ice Shelf. Journal of Glaciology, 2021, 67, 58-74.	2.2	4
4	Chapter 7.2 Mount Erebus. Geological Society Memoir, 2021, 55, 695-739.	1.7	15
5	Seismicity and Pn Velocity Structure of Central West Antarctica. Geochemistry, Geophysics, Geosystems, 2021, 22, e2020GC009471.	2.5	7
6	Swell-Triggered Seismicity at the Near-Front Damage Zone of the Ross Ice Shelf. Seismological Research Letters, 2021, 92, 2768-2792.	1.9	14
7	Remote Triggering of Icequakes at Mt. Erebus, Antarctica by Large Teleseismic Earthquakes. Seismological Research Letters, 2021, 92, 2866-2875.	1.9	6
8	Projected Seismic Activity at the Tiger Stripe Fractures on Enceladus, Saturn, From an Analog Study of Tidally Modulated Icequakes Within the Ross Ice Shelf, Antarctica. Journal of Geophysical Research E: Planets, 2021, 126, e2021JE006862.	3.6	7
9	Surfaceâ€Wave Tomography of the Northern Canadian Cordillera Using Earthquake Rayleigh Wave Group Velocities. Journal of Geophysical Research: Solid Earth, 2021, 126, e2021JB021960.	3.4	13
10	Evidence for asthenospheric flow rotation in northwest Canada: insights from shear wave splitting. Geophysical Journal International, 2021, 228, 1780-1792.	2.4	3
11	Seismic Structure of the Antarctic Upper Mantle Imaged with Adjoint Tomography. Journal of Geophysical Research: Solid Earth, 2020, 125, .	3.4	59
12	Teleseismic Scatteredâ€Wave Imaging Using a Largeâ€N Array in the Albuquerque Basin, New Mexico. Seismological Research Letters, 2020, 91, 287-303.	1.9	7
13	The Upper Mantle Structure of Northwestern Canada From Teleseismic Body Wave Tomography. Journal of Geophysical Research: Solid Earth, 2020, 125, e2019JB018837.	3.4	17
14	Seismic evidence for craton chiseling and displacement of lithospheric mantle by the Tintina fault in the northern Canadian Cordillera. Geology, 2020, 48, 1120-1125.	4.4	11
15	Moho Variations across the Northern Canadian Cordillera. Seismological Research Letters, 2020, 91, 3076-3085.	1.9	11
16	A joint inversion of receiver function and Rayleigh wave phase velocity dispersion data to estimate crustal structure in West Antarctica. Geophysical Journal International, 2020, 223, 1644-1657.	2.4	11
17	Prominent thermal anomalies in the mantle transition zone beneath the Transantarctic Mountains. Geology, 2020, 48, 748-752.	4.4	5
18	P- and S-wave velocity structure of central West Antarctica: Implications for the tectonic evolution of the West Antarctic Rift System. Earth and Planetary Science Letters, 2020, 546, 116437.	4.4	15

#	Article	IF	CITATIONS
19	The Mackenzie Mountains EarthScope Project: Studying Active Deformation in the Northern North American Cordillera from Margin to Craton. Seismological Research Letters, 2020, 91, 521-532.	1.9	10
20	Glacial Earthquakes and Precursory Seismicity Associated With Thwaites Glacier Calving. Geophysical Research Letters, 2020, 47, e2019GL086178.	4.0	12
21	Ross Ice Shelf Icequakes Associated With Ocean Gravity Wave Activity. Geophysical Research Letters, 2019, 46, 8893-8902.	4.0	25
22	Interrogating a Surging Glacier With Seismic Interferometry. Geophysical Research Letters, 2019, 46, 8162-8165.	4.0	5
23	The uppermost mantle seismic velocity structure of West Antarctica from Rayleigh wave tomography: Insights into tectonic structure and geothermal heat flow. Earth and Planetary Science Letters, 2019, 522, 219-233.	4.4	18
24	Spatiotemporal Analysis of the Foreshock–Mainshock–Aftershock Sequence of the 6 July 2017 MwÂ5.8 Lincoln, Montana, Earthquake. Seismological Research Letters, 2019, 90, 131-139.	1.9	6
25	Mapping Crustal Shear Wave Velocity Structure and Radial Anisotropy Beneath West Antarctica Using Seismic Ambient Noise. Geochemistry, Geophysics, Geosystems, 2019, 20, 5014-5037.	2.5	10
26	Seasonal and spatial variations in the ocean-coupled ambient wavefield of the Ross Ice Shelf. Journal of Glaciology, 2019, 65, 912-925.	2.2	12
27	Tidal and Thermal Stresses Drive Seismicity Along a Major Ross Ice Shelf Rift. Geophysical Research Letters, 2019, 46, 6644-6652.	4.0	29
28	Heterogeneous upper mantle structure beneath the Ross Sea Embayment and Marie Byrd Land, West Antarctica, revealed by P-wave tomography. Earth and Planetary Science Letters, 2019, 513, 40-50.	4.4	23
29	Rank Deficiency and Ill-Conditioning. , 2019, , 55-91.		3
30	Tikhonov Regularization. , 2019, , 93-134.		3
31	Discretizing Inverse Problems Using Basis Functions. , 2019, , 135-149.		0
32	Iterative Methods. , 2019, , 151-179.		2
33	Sparsity Regularization and Total Variation Techniques. , 2019, , 181-209.		1
34	Fourier Techniques. , 2019, , 211-233.		0
35	Nonlinear Regression. , 2019, , 235-256.		1
36	Nonlinear Inverse Problems. , 2019, , 257-278.		53

#	Article	IF	CITATIONS
37	Bayesian Methods. , 2019, , 279-306.		4
38	Patients treated with oxaliplatin are at risk for thrombocytopenia caused by multiple drug-dependent antibodies. Blood, 2018, 131, 1486-1489.	1.4	17
39	Multiyear Shallow Conduit Changes Observed With Lava Lake Eruption Seismograms at Erebus Volcano, Antarctica. Journal of Geophysical Research: Solid Earth, 2018, 123, 3178-3196.	3.4	12
40	Measuring Mountain River Discharge Using Seismographs Emplaced Within the Hyporheic Zone. Journal of Geophysical Research F: Earth Surface, 2018, 123, 210-228.	2.8	20
41	Upperâ€Crustal Shearâ€Wave Velocity Structure of the Southâ€Central Rio Grande Rift above the Socorro Magma Body Imaged with Ambient Noise by the Largeâ€N Sevilleta Seismic Array. Seismological Research Letters, 2018, 89, 1708-1719.	1.9	12
42	Seismic evidence for lithospheric foundering beneath the southern Transantarctic Mountains, Antarctica. Geology, 2018, 46, 71-74.	4.4	44
43	The 2015 Sevilleta Socorro Magma Body Mixedâ€Mode Seismic Experiment. Seismological Research Letters, 2018, 89, 1916-1922.	1.9	3
44	Ocean-excited plate waves in the Ross and Pine Island Glacier ice shelves. Journal of Glaciology, 2018, 64, 730-744.	2.2	15
45	Nearâ€Surface Environmentally Forced Changes in the Ross Ice Shelf Observed With Ambient Seismic Noise. Geophysical Research Letters, 2018, 45, 11,187.	4.0	21
46	The nature and evolution of mantle upwelling at Ross Island, Antarctica, with implications for the source of HIMU lavas. Earth and Planetary Science Letters, 2018, 498, 38-53.	4.4	42
47	The Crust and Upper Mantle Structure of Central and West Antarctica From Bayesian Inversion of Rayleigh Wave and Receiver Functions. Journal of Geophysical Research: Solid Earth, 2018, 123, 7824-7849.	3.4	78
48	Observed rapid bedrock uplift in Amundsen Sea Embayment promotes ice-sheet stability. Science, 2018, 360, 1335-1339.	12.6	147
49	Links between atmosphere, ocean, and cryosphere from two decades of microseism observations on the Antarctic Peninsula. Journal of Geophysical Research F: Earth Surface, 2017, 122, 153-166.	2.8	18
50	Tsunami and infragravity waves impacting <scp>A</scp> ntarctic ice shelves. Journal of Geophysical Research: Oceans, 2017, 122, 5786-5801.	2.6	35
51	The uppermost mantle seismic velocity and viscosity structure of central West Antarctica. Earth and Planetary Science Letters, 2017, 472, 38-49.	4.4	29
52	Spatiotemporal evolution of the 2011 Prague, Oklahoma, aftershock sequence revealed using subspace detection and relocation. Geophysical Research Letters, 2017, 44, 7149-7158.	4.0	17
53	Glacial seismology. Reports on Progress in Physics, 2017, 80, 126801.	20.1	66
54	Crustal structure of the Transantarctic Mountains, Ellsworth Mountains and Marie Byrd Land, Antarctica: constraints on shear wave velocities, Poisson's ratios and Moho depths. Geophysical Journal International, 2017, 211, 1328-1340.	2.4	23

#	Article	lF	CITATIONS
55	Upper mantle structure of central and West Antarctica from array analysis of Rayleigh wave phase velocities. Journal of Geophysical Research: Solid Earth, 2016, 121, 1758-1775.	3.4	84
56	A great thermal divergence in the mantle beginning 2.5ÂGa: Geochemical constraints from greenstone basalts and komatiites. Geoscience Frontiers, 2016, 7, 543-553.	8.4	137
57	Crustal and upper-mantle structure beneath ice-covered regions in Antarctica from <i>S</i> -wave receiver functions and implications for heat flow. Geophysical Journal International, 2016, 204, 1636-1648.	2.4	36
58	Strong seismic scatterers near the core–mantle boundary north of the Pacific Anomaly. Physics of the Earth and Planetary Interiors, 2016, 253, 21-30.	1.9	16
59	Ice shelf structure derived from dispersion curve analysis of ambient seismic noise, Ross Ice Shelf, Antarctica. Geophysical Journal International, 2016, 205, 785-795.	2.4	40
60	A seismic transect across West Antarctica: Evidence for mantle thermal anomalies beneath the Bentley Subglacial Trench and the Marie Byrd Land Dome. Journal of Geophysical Research: Solid Earth, 2015, 120, 8439-8460.	3.4	54
61	Ross ice shelf vibrations. Geophysical Research Letters, 2015, 42, 7589-7597.	4.0	52
62	The mantle transition zone beneath <scp>W</scp> est <scp>A</scp> ntarctica: Seismic evidence for hydration and thermal upwellings. Geochemistry, Geophysics, Geosystems, 2015, 16, 40-58.	2.5	38
63	Multiple scattering from icequakes at Erebus volcano, Antarctica: Implications for imaging at glaciated volcanoes. Journal of Geophysical Research: Solid Earth, 2015, 120, 1129-1141.	3.4	23
64	Reactivated faulting near Cushing, Oklahoma: Increased potential for a triggered earthquake in an area of United States strategic infrastructure. Geophysical Research Letters, 2015, 42, 8328-8332.	4.0	59
65	Hundreds of Earthquakes per Day: The 2014 Guthrie, Oklahoma, Earthquake Sequence. Seismological Research Letters, 2015, 86, 1318-1325.	1.9	49
66	The Seismic Noise Environment of Antarctica. Seismological Research Letters, 2015, 86, 431-431.	1.9	1
67	The Seismic Noise Environment of Antarctica. Seismological Research Letters, 2015, 86, 89-100.	1.9	50
68	Data Quality of Collocated Portable Broadband Seismometers Using Direct Burial and Vault Emplacement. Bulletin of the Seismological Society of America, 2015, 105, 2420-2432.	2.3	19
69	Upstairs-downstairs: supercontinents and large igneous provinces, are they related?. International Geology Review, 2015, 57, 1341-1348.	2.1	64
70	The crustal thickness of West Antarctica. Journal of Geophysical Research: Solid Earth, 2014, 119, 378-395.	3.4	103
71	Upper mantle seismic anisotropy beneath the West Antarctic Rift System and surrounding region from shear wave splitting analysis. Geophysical Journal International, 2014, 198, 414-429.	2.4	27
72	Imaging the Antarctic mantle using adaptively parameterized P-wave tomography: Evidence for heterogeneous structure beneath West Antarctica. Earth and Planetary Science Letters, 2014, 408, 66-78.	4.4	76

#	Article	IF	CITATIONS
73	Seismic tomography of the Colorado Rocky Mountains upper mantle from CREST: Lithosphere–asthenosphere interactions and mantle support of topography. Earth and Planetary Science Letters, 2014, 402, 107-119.	4.4	13
74	Antarctic icequakes triggered by the 2010 Maule earthquake in Chile. Nature Geoscience, 2014, 7, 677-681.	12.9	44
75	Multi-scale reasonable attenuation tomography analysis (MuRAT): An imaging algorithm designed for volcanic regions. Journal of Volcanology and Geothermal Research, 2014, 277, 22-35.	2.1	20
76	Refinement of the supercontinent cycle with Hf, Nd and Sr isotopes. Geoscience Frontiers, 2013, 4, 667-680.	8.4	75
77	Seismic detection of an active subglacial magmatic complex in Marie Byrd Land, Antarctica. Nature Geoscience, 2013, 6, 1031-1035.	12.9	55
78	Multiple fluvial processes detected by riverside seismic and infrasound monitoring of a controlled flood in the Grand Canyon. Geophysical Research Letters, 2013, 40, 4858-4863.	4.0	90
79	A rootless rockies—Support and lithospheric structure of the Colorado Rocky Mountains inferred from CREST and TA seismic data. Geochemistry, Geophysics, Geosystems, 2013, 14, 2670-2695.	2.5	65
80	Internal structure of Erebus volcano, Antarctica imaged by highâ€resolution activeâ€source seismic tomography and coda interferometry. Journal of Geophysical Research: Solid Earth, 2013, 118, 1067-1078.	3.4	30
81	The first second of volcanic eruptions from the Erebus volcano lava lake, Antarctica—Energies, pressures, seismology, and infrasound. Journal of Geophysical Research: Solid Earth, 2013, 118, 3318-3340.	3.4	55
82	Expecting the Unexpected: Black Swans and Seismology. Seismological Research Letters, 2012, 83, 5-6.	1.9	9
83	Imaging of Erebus volcano using body wave seismic interferometry of Strombolian eruption coda. Geophysical Research Letters, 2012, 39, .	4.0	24
84	Efficient stochastic estimation of the model resolution matrix diagonal and generalized cross–validation for large geophysical inverse problems. Journal of Geophysical Research, 2011, 116, .	3.3	32
85	Episodic zircon ages, Hf isotopic composition, and the preservation rate of continental crust. Bulletin of the Geological Society of America, 2011, 123, 951-957.	3.3	214
86	Small-scale convection at the edge of the Colorado Plateau: Implications for topography, magmatism, and evolution of Proterozoic lithosphere. Geology, 2010, 38, 611-614.	4.4	149
87	Kinematic and seismic analysis of giant tabular iceberg breakup at Cape Adare, Antarctica. Journal of Geophysical Research, 2010, 115, .	3.3	32
88	Seismic Tomography of Erebus Volcano, Antarctica. Eos, 2010, 91, 53-55.	0.1	5
89	Global trends in extremal microseism intensity. Geophysical Research Letters, 2010, 37, .	4.0	52
90	Highâ€resolution receiver function imaging reveals Colorado Plateau lithospheric architecture and mantleâ€supported topography. Geophysical Research Letters, 2010, 37, .	4.0	15

#	Article	IF	CITATIONS
91	Episodic zircon age spectra of orogenic granitoids: The supercontinent connection and continental growth. Precambrian Research, 2010, 180, 227-236.	2.7	398
92	Evidence and implications for a widespread magmatic shutdown for 250ÂMy on Earth. Earth and Planetary Science Letters, 2009, 282, 294-298.	4.4	252
93	Grand Challenges for Seismology. Eos, 2009, 90, 361-362.	0.1	14
94	Zircon Age Episodicity and Growth of Continental Crust. Eos, 2009, 90, 364-364.	0.1	38
95	Seismic observations of glaciogenic ocean waves (micro-tsunamis) on icebergs and ice shelves. Journal of Glaciology, 2009, 55, 193-206.	2.2	58
96	Infrasonic tracking of large bubble bursts and ash venting at Erebus Volcano, Antarctica. Journal of Volcanology and Geothermal Research, 2008, 177, 661-672.	2.1	50
97	Acoustic source characterization of impulsive Strombolian eruptions from the Mount Erebus lava lake. Journal of Volcanology and Geothermal Research, 2008, 177, 673-686.	2.1	73
98	Moment tensor inversion of very long period seismic signals from Strombolian eruptions of Erebus Volcano. Journal of Volcanology and Geothermal Research, 2008, 177, 635-647.	2.1	52
99	Seismic and hydroacoustic tremor generated by colliding icebergs. Journal of Geophysical Research, 2008, 113, .	3.3	74
100	Multidecadal Climate-induced Variability in Microseisms. Seismological Research Letters, 2008, 79, 194-202.	1.9	121
101	Characteristics of the October 2005 Microearthquake Swarm and Reactivation of Similar Event Seismic Swarms over Decadal Time Periods near Socorro, New Mexico. Bulletin of the Seismological Society of America, 2008, 98, 93-105.	2.3	19
102	Transoceanic wave propagation links iceberg calving margins of Antarctica with storms in tropics and Northern Hemisphere. Geophysical Research Letters, 2006, 33, .	4.0	101
103	Lithospheric structure of the Rio Grande rift. Nature, 2005, 433, 851-855.	27.8	78
104	Relative partitioning of acoustic and seismic energy during Strombolian eruptions. Journal of Volcanology and Geothermal Research, 2005, 148, 334-354.	2.1	99
105	Monitoring rapid temporal change in a volcano with coda wave interferometry. Geophysical Research Letters, 2005, 32, .	4.0	98
106	Seismic imaging of the crust and upper mantle using regularized joint receiver functions, frequency–wave number filtering, and multimode Kirchhoff migration. Journal of Geophysical Research, 2005, 110, .	3.3	49
107	Imaging the seismic structure of the crust and upper mantle beneath the Great Plains, Rio Grande Rift, and Colorado Plateau using receiver functions. Journal of Geophysical Research, 2005, 110, .	3.3	80
108	Crust and upper mantle shear wave structure of the southwest United States: Implications for rifting and support for high elevation. Journal of Geophysical Research, 2004, 109, .	3.3	80

#	Article	IF	CITATIONS
109	Upper mantle convection beneath the central Rio Grande rift imaged byPandSwave tomography. Journal of Geophysical Research, 2004, 109, .	3.3	87
110	Volcanic eruptions observed with infrasound. Geophysical Research Letters, 2004, 31, .	4.0	101
111	Interpretation and utility of infrasonic records from erupting volcanoes. Journal of Volcanology and Geothermal Research, 2003, 121, 15-63.	2.1	77
112	Shear wave splitting and mantle flow beneath LA RISTRA. Geophysical Research Letters, 2003, 30, .	4.0	22
113	Using Automated, High-precision Repicking to Improve Delineation of Microseismic Structures at the Soultz Geothermal Reservoir. , 2002, 159, 563-596.		78
114	Using Automated, High-precision Repicking to Improve Delineation of Microseismic Structures at the Soultz Geothermal Reservoir. , 2002, , 563-596.		2
115	Seismic and acoustic observations at Mount Erebus Volcano, Ross Island, Antarctica, 1994–1998. Journal of Volcanology and Geothermal Research, 2000, 101, 105-128.	2.1	105
116	Automatic Phase Pick Refinement and Similar Event Association in Large Seismic Datasets. Modern Approaches in Geophysics, 2000, , 231-263.	0.1	22
117	Current status of seismic and borehole measurements for HDR/HWR development. Geothermics, 1999, 28, 475-490.	3.4	25
118	Broadband recording of Strombolian explosions and associated very-long-period seismic signals on Mount Erebus Volcano, Ross Island, Antarctica. Geophysical Research Letters, 1998, 25, 2297-2300.	4.0	98
119	A comparison of select trigger algorithms for automated global seismic phase and event detection. Bulletin of the Seismological Society of America, 1998, 88, 95-106.	2.3	412
120	A lower crustal extension to a midcrustal magma body in the Rio Grande Rift, New Mexico. Journal of Geophysical Research, 1996, 101, 25283-25291.	3.3	33
121	High-frequency analysis of seismic background noise as a function of wind speed and shallow depth. Bulletin of the Seismological Society of America, 1996, 86, 1507-1515.	2.3	137
122	Small-scale stress heterogeneity in the Anza seismic gap, southern California. Journal of Geophysical Research, 1994, 99, 6801.	3.3	23
123	Comprehensive characterization of waveform similarity in microearthquake data sets. Bulletin of the Seismological Society of America, 1993, 83, 1307-1314.	2.3	84
124	Initial shear wave particle motions and stress constraints at the Anza Seismic Network. Geophysical Journal International, 1992, 108, 740-748.	2.4	47
125	High-frequency borehole seismograms recorded in the San Jcinto Fault zone, Southern California Part 2. Attenuation and site effects. Bulletin of the Seismological Society of America, 1991, 81, 1081-1100.	2.3	74
126	Quantitative measurements of shear wave polarizations at the Anza Seismic Network, southern California: Implications for shear wave splitting and earthquake prediction. Journal of Geophysical Research, 1990, 95, 12449-12473.	3.3	147

#	Article	IF	CITATIONS
127	Shear-wave anisotropy of active tectonic regions via automated S-wave polarization analysis. Tectonophysics, 1989, 165, 279-292.	2.2	70